

Three-dimensional dynamic bipedal walking based on passive dynamic walking mechanism using telescopic knee via phase oscillator with ground reaction force

Tetsuya Kinugasa¹ · Tomoki Tada¹ · Yuki Yokoyama¹ · Koji Yoshida¹ · Ryota Hayashi¹ · Shinsaku Fujimoto¹

Received: 4 April 2018 / Accepted: 8 November 2018 / Published online: 26 November 2018
© ISAROB 2018

Abstract

This study aims to generate 3-D dynamic bipedal walking using two oscillators of a CPG approach based on its body dynamics. First, a 3-D biped, which inherited the aspect of the previous passive dynamic walker, was developed that contained flat feet with pressure sensors, ankle joints composed of ball joints surrounded by coil springs, telescopic knees, and actuated hip joints using a direct drive (DD) motor. The torso was controlled by the DD motors using a PD control scheme. Next, the Owaki–Ishiguro method was used with ground contact information in the phase oscillator to the knee joint. Finally, experimental tests were conducted to elucidate the effectiveness of the biped. A 3-D dynamic bipedal gait of RW06 was developed using knee oscillation based on the phase oscillator. Bipedal walking was excited only by the knee oscillation; therefore, the gait was strongly affected by the body dynamics.

Keywords Central pattern generator · Phase oscillator · Bipedal walking · 3-D dynamic walking

1 Introduction

Passive dynamic walking [1] has emerged using the body dynamics of a biped and the interaction between the body and environment. Passive dynamic walking can be used to create a natural and an energy-efficient gait by adapting to the environment according to the body dynamics. Methods that create dynamic walking while gradually adding active elements to a biped to achieve the passive dynamic walking can generate bipedal walking using the body dynamics, i.e., the bipedal gait inherits the aspect of the passive dynamic walking. However, the passive dynamic walking and the gradually adding strategy are not robust against disturbances mainly from the environment.

Conversely, a central pattern generator (CPG), obtained from biological findings, was introduced to control legged

robots, and achieved various adaptive and robust locomotion including bipeds [2–5]. Some studies showed possibility of an adaptive three-dimensional (3-D) bipedal walking [5]; however, there was not a systematic design strategy for the coordination of the oscillators, except for the studies of multi-legged robots by Owaki and Ishiguro [6–11]. In addition, the CPG signal was used only for the desired trajectory of the tracking control of the joints. The trajectory tracking control for the joints may neglect the body dynamics for the locomotion. Thus, Hanamoto et al. [8] introduced some passive joints for a quadruped robot to achieve a dynamic locomotion. For the bipedal walking, the body is fundamentally supported by a foot and the center of the total mass is outside of the foot print when the biped walks dynamically. Therefore, it is challenging to achieve a 3-D, dynamic, adaptive, and robust bipedal gait using the body dynamics.

This study aimed to generate 3-D dynamic bipedal walking using two oscillators of a CPG approach based on its body dynamics. First, a 3-D biped, referred to as RW06, was developed, which had two legs and a torso between the legs. The torso was controlled by the DD motors using a proportional and derivative (PD) control scheme. Next, the Owaki–Ishiguro approach [10] was used with the ground contact information in the phase oscillator for the knee joint. Finally, experimental tests were conducted to determine the

This work was presented in part at the 23rd International Symposium on Artificial Life and Robotics, Beppu, Oita, January 18–20, 2018.

✉ Tetsuya Kinugasa
kinugasa@mech.ous.ac.jp

¹ Okayama University of Science, 1-1 Ridai-cho, Kita-ku, Okayama, Japan

effectiveness of the biped. A 3-D dynamic bipedal gait of RW06 was developed using knee oscillation based on the phase oscillator. Bipedal walking was excited only by the knee oscillation; therefore, the gait was strongly affected by the body dynamics.

2 3-D bipedal walker

A 3-D biped with ankle springs and flat feet, RW03, was developed, and a 3-D passive dynamic walking gait [12] was achieved. A telescopic knee joint was added to RW03, and developed the 3-D bipeds, RW04 and RW05, were developed. The 3-D dynamic bipedal gait for the bipeds on a horizontal surface using a forced oscillation by the knee joint [13, 14] was obtained. In this section, a new biped, ‘RW06’ with hip actuators based on the previous bipeds is discussed.

2.1 RW06

Figure 1 shows the 3-D dynamic biped, RW06. RW06 had a height of 900 mm and a total weight of 6.4 kg. The center of the total mass was 450 mm from the ground, and the eigenfrequencies were 4.3 rad/s for the swing leg and 5.1 rad/s for the biped in the frontal plane, which were inherent characteristics of the previous bipeds (Table 1). The DD motor was implemented in the hip joint for back-drivable actuation, as shown in Fig. 2 (top left). The DD motor, MDH-4012, was made by Micro-Tech Laboratory Co. Ltd., and provided a maximum instantaneous torque of 0.6 Nm. The biped had two legs and a torso between the legs. The DD motor could create free oscillation of the hip joints using back-drivability and could generate an appropriate torque for walking, simultaneously. Therefore, torque control was

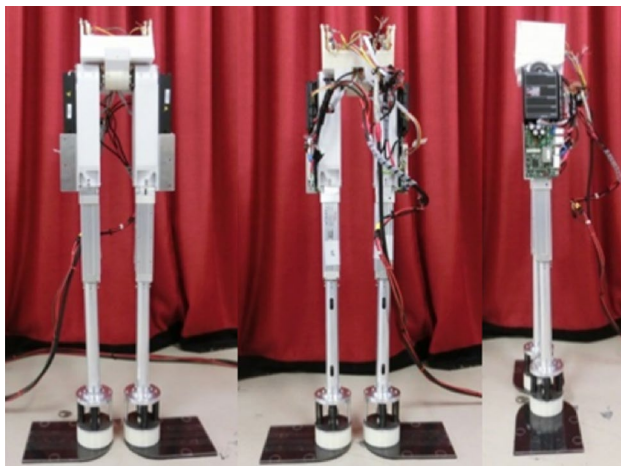


Fig. 1 RW06 frontal view (left), rear view (center), and left-side view (right)

Table 1 Specification of RW06

Total mass	6.4 kg
Height	900 mm
CoG position from the ground	450 mm
Eigenfrequency of swing leg	4.3 rad/s
Eigenfrequency about roll axis*	5.1 rad/s

*Frequency of the biped in frontal plane

ensured for the hip joints instead of usual trajectory tracking. The top right and bottom of Fig. 2 shows pressure sensors attached to the foot sole. There were three pressure sensors for each foot; however, the front one was used to detect the ground reaction force.

2.2 Walking via sinusoidal oscillation

Oscillation from a joint is necessary to excite a bipedal gait based on the oscillation characteristic of the body. Previously, the 3-D bipedal gait was excited using the sinusoidal oscillation of a telescopic knee joint [14]. The oscillated joint was controlled by a trajectory tracking method using the sinusoidal function; however, the other joints were not controlled. The ankle joint was supported by a spherical joint and coil springs. The hip joint was controlled by the DD motor to keep the center position of the legs; thus, the relative angle between the legs could rotate freely. Therefore, the obtained bipedal gait could change based on the body dynamics for the amplitude and frequency of the knee oscillation. The following equations represent the desired trajectory of the knee oscillation:



Fig. 2 DD motor (left, Micro-tech Laboratory, MDH-4012), pressure sensor (right, interlink electronics, FSR402 short), and foot with sensors (bottom)

$$\dot{\zeta} = \omega \quad (1)$$

$$d_{d_i} = A \sin \{\zeta - (i-1)\pi\} + d_0. \quad (2)$$

$i = 1$ and 2 indicate left and right, respectively, and ω is the angular frequency of the knee joint. d_{d_i} is the desired trajectory of the knee and d_0 is the center of the oscillation. A is the amplitude of the knee. The desired trajectory of the knee joint is a harmonic wave, and the phase difference between the knees is 180° , which is given explicitly in Eq. (2). The tracking control scheme was a PD control given by the following equation:

$$u_{ki} = -K_p(d_i - d_{d_i}) - K_d(\dot{d}_i - \dot{d}_{d_i}), \quad (3)$$

where u_{ki} is the input for the knee actuator, d_i is the displacement of the knee, and K_p and K_d are the proportional and derivative gains for the PD control, respectively. In addition, the DD motor was used as the hip joint, and controlling the absolute orientation of the torso was controlled using the following PD control scheme:

$$u_{hi} = -K_{hp}\alpha - K_{hd}\dot{\alpha}, \quad (4)$$

where u_{hi} is the hip joint torque, α is the hip joint defined by the relative angle between the legs, and K_{hp} and K_{hd} are the proportional and derivative gains of the PD control, respectively. The desired position of the body was set to the center of the legs.

2.3 Phase oscillator with a ground reaction force

The previous method using the sinusoidal oscillation was extended to the phase oscillator based on the Owaki–Ishiguro approach. The approach could be straightforwardly extended from the sinusoidal oscillation. The approach uses the ground reaction force to remain a stance leg when the foot touches to the ground. Equations (1), and (2) were extended to the phase oscillator and are given by the following equations:

$$\dot{\zeta}_i = \omega - \sigma N_i \cos \zeta_i, \quad (5)$$

$$d_{d_i} = -A \sin \zeta_i + d_0. \quad (6)$$

Equation (5) shows the phase oscillator [10], where N_i indicates the ground reaction force measured by the i th pressure sensor, as shown in Fig. 2 (right). We used the front sensor of each foot only, and thus, i means the number of the front sensor. σ is positive weight for the ground reaction force. Equation (6) shows the desired trajectory for the knee oscillation.

When the sole of the foot felt the reaction force (contacted to the ground), $N_i > 0$, and the weight σ was large enough, $\zeta_i = 3\pi/2$ is a stable equilibrium point. Therefore, the knee, given by Eqs. (5) and (6), had tendency to remain in the

extended position, $\zeta_i = 3\pi/2$, when the foot detected the ground reaction force. It was expected that the bipedal gait was excited by the knee oscillation changing the phase with the ground reaction force. The knees started the oscillation for the initial phase difference of zero. When the ground reaction force in Eq. (5) provided pressure alternately, e.g., an external oscillation was given, then the knee frequency of the stance leg decreased owing to the second term of Eq. (5). The phase of the stance knee was delayed relative to the swing knee around the extended position. Finally, the phase difference converged to 180° approximately caused by the interaction between the robot and the ground.

3 Experiment

We conducted experimental tests for bipedal walking using RW06 based on the phase oscillator with a ground reaction force. The parameters in Eq. (5) were given as follows: the weight $\sigma = 0.9$ to 1.2 , the angular frequency $\omega = 0.9$ Hz, and the amplitude $A = 8$ mm. In the domain of the weight, RW06 could walk stably. The weight was heuristically given and the other parameters were based on those of the previous experiment using sinusoidal oscillation [14]. In the experiment, a forced oscillation, an alternate motion to the left and right directions, was applied to RW06 for the first several steps to provide alternative ground reaction force to the foot soles by an external force. Figure 3 shows the hip joint angle. The walking angle defined by the hip joint angle at the double support phase reached approximately 13° in the first three steps, and RW06 walked 23 steps with some variation. Because of the limitation of the tether length and the lab area, the knee oscillation was stopped after 23 step. Figure 4 shows sequential screenshots of 3-D bipedal gait by RW06. RW06 walked stably with a slight oscillation in the lateral direction. In the figure, you can find a person

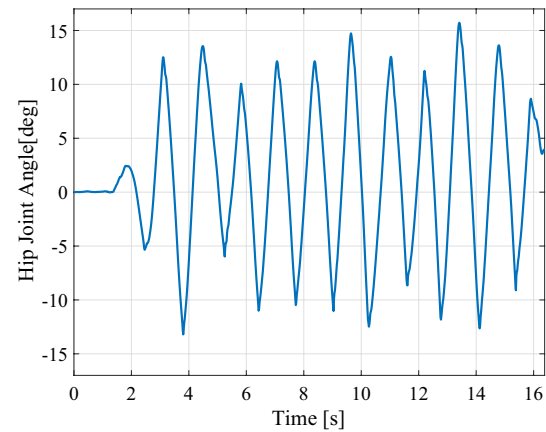


Fig. 3 Hip joint angle ($\sigma = 0.9$)

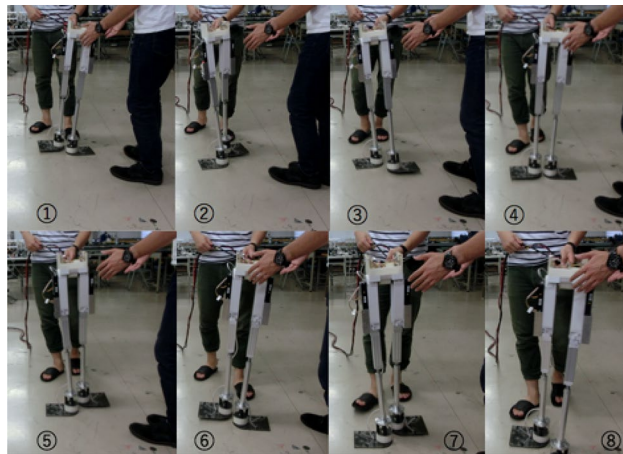


Fig. 4 Sequential screenshots of the 3-D bipedal gait by RW06

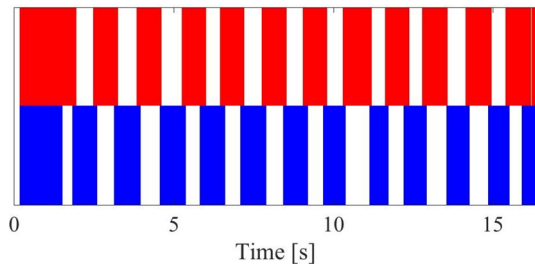


Fig. 5 Gait diagram

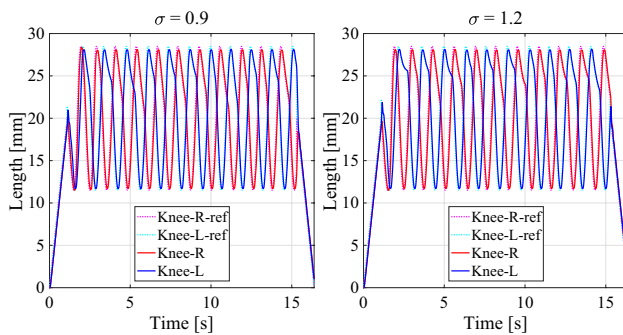


Fig. 6 Knee displacement

who tried to support RW06. He did not touch RW06 in the test, who was just preparing to catch RW06 when it tended to tumble. Figure 5 shows a gait diagram. The red and blue areas indicate the stance phase of the left and right legs, respectively. The left and right stance phases overlapped at the beginning and in the end of each step; and thus, RW06 achieved a bipedal gait. Figure 6 shows the displacements and desired trajectories of the left and right knee joints for the weights σ of 0.9 (left) and 1.2 (right). The magenta and cyan dotted lines indicate the desired trajectory of the

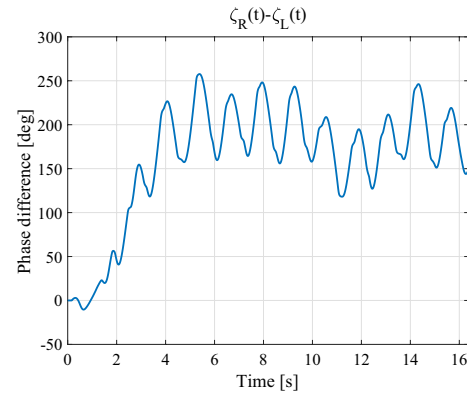


Fig. 7 Phase difference of the knee joint ($\sigma = 0.9$)

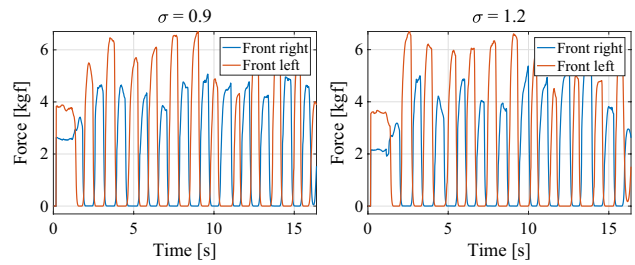


Fig. 8 Outputs of the force sensors located on the front left and right of the sole

right and left knee joints, respectively. The red and blue lines indicate the displacement of the right and left knee joints, respectively. After the knee joints initially expanded to the center of the oscillation $d_0 = 20$ mm, the oscillations started with the same initial phase, i.e., the phase difference of zero, using the control scheme given by Eqs. (5) and (6). The phases of the desired trajectory started at the coordinate phase and changed to the opposite phase in the first three steps. As mentioned previously, a forced oscillation was provided for the first several steps (four steps). After the oscillation converged to an approximately steady motion, the knee joints remained or evolved slowly at the maximum, i.e., the extended position. The tendency was more pronounced for the weight of 1.2. The phase did not stop and increased monotonously, because the weight σ was not relatively large. Figure 7 shows the time evolution of the phase difference. The phase difference oscillated at approximately 200° with the amplitude of 50° . The oscillation was possibly provided by the decrease in the angular frequency owing to the ground reaction force. This oscillation of the phase difference could maintain the behavior when the knee was extended. Figure 8 shows the forces of the pressure sensors put on the left and right soles. Three pressure sensors were placed on the feet, as shown in Fig. 2. Because the forces measured by the sensors located on the rear side were small, The ground reaction

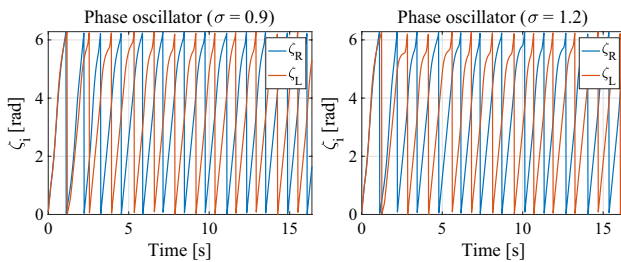


Fig. 9 Phase for the knees

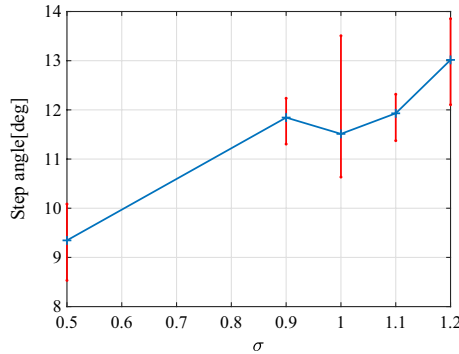


Fig. 10 Step angle with respect to weight σ

force measured by the front sensors was used, as mentioned previously. The ground reaction force had the same tendency in any cases. Figure 9 shows the time response of the knee phase. The blue and red lines indicate experimental results for $\sigma = 0.9$ and 1.2, respectively. For the weight of 0.9, the inclination, i.e., the time derivation, of the phase around 5.5 rad was smaller, which meant that the phase evolved slowly. For the weight of 1.2, the tendency was more pronounced, e.g., for $t = 3$ and 5, the phase was approaching to the horizontal. Therefore, the knee was maintained in the extended position, $\zeta_i = 5 \approx 3/\pi$. The knee rapidly contracted when the phase returned to a steady oscillation when the foot did not sense the ground reaction force. Therefore, the interaction between the foot and the ground and the sensory feedback of the oscillator for appropriate weights provided the autonomous coordination for the left and right knees. The walking angle became longer when the weight is larger, because the stance phase was maintained longer than the swing phase. To illustrate the tendency, the variation of the walking angle with respect to the weight $0.5 \leq \sigma \leq 1.2$ is shown in Fig. 10. For the weight of 0.5, RW06 could walk. However, it was need to support when it tended sometimes to tumble. In the case, the results were rejected from the data. The blue line and marks indicate the average of the walking angle for three tests, and the red line and marks indicate the maximum and minimum values, respectively. Thus, the walking angle increased when the weight increased.



Fig. 11 RW06 walks on a gentle ascent

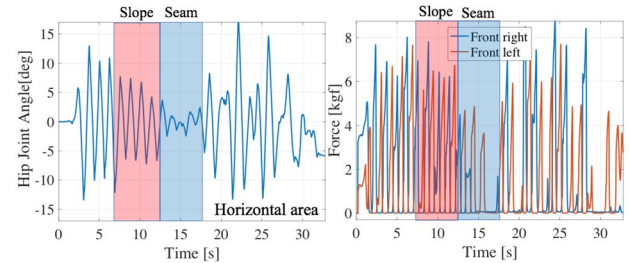


Fig. 12 Hip joint angle and ground reaction force when RW06 could walk on a gentle ascent

Finally, we conducted performance tests that evaluated a kind of adaptability, climb-ability, for a gentle ascent. The angle of the ascent was 1.5° and the weight of 0.9 for the phase oscillator was used for the tests. Two horizontal areas were connected to the slope. From Fig. 11, RW06 could climb the gentle ascent. The left figure of Fig. 12 shows the hip joint angle. The walking angle decreases around 7 s, it keeps the small walking angle of 7° until 13 s (red area), and RW06 steps on the same area from 13 s to 17 s (blue area). RW06 started climbing around 7 s and approached to the horizontal area around 13 s. After several stepping, it started walking forward again on the horizontal area, even though the walking angle was oscillatory. To clarify the foot stepping, the ground reaction forces of the both foot are shown in the right of Fig. 12. The ground reaction forces also decreased when RW06 started climbing, and it was lost, especially for the right sensor when RW06 approached to the horizontal area (blue area). The force sensors located at the front of sole did not contact to the ground in the area where the slope angle discretely changed from 1.5° to 0°. In the horizontal area, the ground reaction force was also oscillatory. The horizontal area was put on the floor that was not flat; thus, the area was trembled because of the movement of RW06. We also conducted some experimental tests using the sinusoidal knee oscillation to compare the performance of the both methods, however, RW06 could not complete to climb the same slope. Therefore, we can conclude that the

phase oscillator using the ground reaction force had adaptability against gentle ascent.

4 Conclusions

In this study, a 3-D biped RW06 was developed and a 3-D dynamic bipedal gait was created. Knee oscillation was designed based on a phase oscillator with a ground reaction force. The gait was generated using body dynamics, because the degrees of freedom of the biped, excepting the knees and torso, were passive. The previous strategy using a simple sinusoid explicitly required a phase difference of 180°; however, the phase oscillator automatically provided the phase difference using the ground reaction force. Moreover, the bipedal gait provided by the phase oscillator had an adaptability against a gentle ascent. It was important that the 3-D gait was emerged only by the phase oscillator of the knee joint and the body dynamics. The gait variation for the angular frequency, amplitude, ground reaction force, etc. will be determined, and the adaptability of the bipedal gait will be verified.

Acknowledgements This work was partly supported by JSPS KAKENHI Nos. 26420215 and 17K06281.

References

1. McGeer T (1988) Passive dynamic walking. CSS-IS TR 88-02
2. Taga G (1991) Self-organized control of bipedal locomotion by neural oscillators in unpredictable environment. *Biol Cybern* 65(3):147–159
3. Geyer H, Herr H (2010) A muscle-reflex model that encodes principles of legged mechanics produces human walking dynamics and muscle activities. *IEEE Trans Neural Syst Rehabil Eng* 18(3):263–273
4. Yamasaki T (2003) Phase reset and dynamic stability during human gait. *BioSystem* 71(1–2):221–232
5. Aoi S, Tsuchiya K (2005) Locomotion control of a biped robot using nonlinear oscillators. *Auton Robot* 19(3):219–232
6. Horikita S et al (2016) Adaptive bipedal walking control based on “TEGOTAE function”. In: Proc. of 28th Symposium on decentralize system, pp. 116–119
7. Yashitani N et al (2016) On implicit and explicit control mechanism in rocking-induced tripodal walking robot. In: Proc. of ROBOMECH 2016. 2A2-08a6
8. Hamamoto M et al (2016) Gait analysis of quadruped robot focus on body structure. In: Proc. of ROBOMECH 2016, 1A1-C10
9. Owaki D, Ishiguro A (2017) A quadruped robot exhibiting spontaneous gait transitions from walking to trotting to galloping. *Sci Rep* 7:277
10. Owaki D (2017) A minimal model describing hexapedal interlimb coordination: the Tegotae-based approach. *Front Neurorobotics* 11:29
11. Kano T, Sakai K, Yasui K, Owaki D, Ishiguro A (2017) Decentralized control mechanism underlying interlimb coordination of millipedes. *Bioinspiration Bio-mimetics* 12:036007
12. Kinugasa T (2009) 3D Passive walker with ankle springs and flat feet. *J Robot Soc Jpn* 27(10):1169–1172
13. Kinugasa T (2015) 3D Dynamic biped walker with flat feet and ankle springs: passive gait analysis and extension to active walking. *J Robot Mechatron* 27(4):444–452
14. Kinugasa T (2015) Development of a three-dimensional dynamic biped walking via the oscillation of telescopic knee joint and its gait analysis. *J Mech Eng Sci* 9:1529–1537